JOURNAL OF BACTERIOLOGY, Mar. 1996, p. 1420–1429 Vol. 178, No. 5
0021-9193/96/$04.00+0

Plasmid RK2 Toxin Protein ParE: Purification and Interaction with the ParD Antitoxin Protein

ERIK P. JOHNSON,[1] ARNE R. STRÖM,[2] AND DONALD R. HELINSKI[1]*

Department of Biology and Center for Molecular Genetics, University of California at San Diego, La Jolla, California 92037-0634,[1] and Norwegian College of Fishery Science, University of Tromso, 9000 Tromso, Norway[2]

Received 3 August 1995/Accepted 21 December 1995

The *parDE* operon, located within the 3.2-kb stabilization region of plasmid RK2, encodes antitoxin (ParD) and toxin (ParE) proteins that stabilize the maintenance of this broad-host-range plasmid via a postsegregational killing mechanism. A ParE protein derivative, designated ParE′, was purified by construction of a fusion protein, GST-ParE, followed by glutathione-agarose binding and cleavage of the fusion protein. ParE′ has three additional amino acids on the N terminus and a methionine residue in place of the native leucine residue. The results of glutathione-agarose affinity binding and glutaraldehyde cross-linking indicate that ParE′ exists as a dimer in solution and that it binds to the dimeric form of ParD to form a tetrameric complex. The formation of this complex is presumably responsible for the ability of ParD to neutralize ParE toxin activity. Previous studies demonstrated that the *parDE* operon is autoregulated as a result of the binding of the ParD protein to the *parDE* promoter. ParE′ also binds to the *parDE* promoter but only in the presence of the autoregulatory ParD protein. ParE′, in the presence or absence of the ParD protein, does not bind to any other part of the 3.2-kb stabilization region. The binding of the ParE′ protein to ParD did not alter the DNase I footprint pattern obtained as a result of ParD binding to the *parDE* promoter. The role of ParE in binding along with ParD to the promoter, if any, remains unclear.

In order for a plasmid to be stably maintained in a bacterial population, each daughter cell must inherit at least one copy of the plasmid upon cell division. For high-copy-number plasmids, random segregation alone may be adequate for achieving stability. Low-copy-number plasmids, however, employ one or more genetic loci which encode mechanisms which stabilize the plasmid within a growing bacterial population (49). Several different plasmid stabilization mechanisms have been identified (19, 31, 56). One such system involves the selective killing of plasmid-free daughter cells of *Escherichia coli*. The *hok*/*sok*, *srnB*, and *pnd* loci of plasmids R1, F, and R483, respectively, encode cytotoxic proteins (Hok, SrnB′, and Pnd, respectively), which cause a "ghost" cell phenotype (14). Expression of the toxin is posttranscriptionally regulated by an antisense RNA, which blocks translation and exhibits a relatively short half-life (13, 15). In a plasmid-free segregant, the unstable antisense RNA is degraded, allowing for translation of the toxins and the subsequent death of the plasmid-free cell (52).

In the case of another family of killing systems (23), which includes the *ccd* locus of F (2, 9, 20, 22, 47, 51), the *parD*/*pem* locus of R1-R100 (4, 5, 39, 54), and the *phd-doc* system of prophage P1 (28), two proteins are involved, a toxin (CcdB, Kis/PemK, and Doc, respectively) and an antitoxin (CcdA, Kid/PemI, and Phd, respectively), which presumably is more susceptible to degradation in a plasmid-free cell (5, 20, 28). CcdA and PemI protein degradation has been shown to be mediated by the Lon protease (53, 55), while Phd degradation is mediated by the ClpXP serine protease (29). Thus, in the absence of the plasmid, sufficiently high levels of antitoxin are not maintained, and the toxin is able to kill the host cell. Cell death is accompanied by filamentation and has been shown for the *ccd* system to be caused by the ability of the CcdB protein to induce the ATP-dependent cleavage of DNA by gyrase (3). In the case of the F *ccd* and R1 *parD* systems, the toxin and antitoxin are transcribed from the same operon, which is autoregulated by the coordinated action of both proteins (9, 39, 51).

RK2 is a broad-host-range plasmid (32) that despite a relatively low copy number of four to seven copies per chromosome (12) is stably maintained in a wide-range of gram-negative bacteria. Stabilization of RK2 is accomplished by at least two genetic regions of the plasmid utilizing different stabilization mechanisms. The *psa* (postsegregational arrest) locus, which has not been mapped, causes the growth inhibition of daughter cells which fail to inherit the plasmid (24). Factors encoded by this region do not appear to be lethal to the host, as plasmid-free segregants recover from growth inhibition several hours after loss of the plasmid.

The second stabilization region is a 3.2-kb sequence, designated the RK2 *par* region, located between 32.6 and 35.8 kb on the RK2 map (16, 35, 42). The 3.2-kb *par* region has been shown to stabilize mini-RK2 replicons in various hosts and in a vector-independent manner (8, 36, 38). It encodes five genes on two divergent operons, *parCBA* and *parDE*. These operons are autoregulated at the transcriptional level by ParA and ParD, respectively (8, 10, 37). ParA has been shown to be a resolvase, acting at an in *cis* site positioned between the two operons (11, 16). While a multimer resolution system can provide stabilization by increasing the effective number of plasmids available for segregation at the time of cell division, the resolvase activity of the *parCBA* operon by itself is insufficient to account for the stabilization of RK2 plasmids. The functions of the products of *parB* and *parC* are not yet known; however, the ParB protein has been shown to exhibit a nuclease activity (17).

A 0.7-kb segment of the 3.2-kb region of RK2 that contains the *parDE* operon has been shown to stabilize mini-RK2 replicons in various *E. coli* strains under various growth conditions

* Corresponding author. Phone: (619) 534-3638. Fax: (619) 534-7073. Electronic mail address: helinski@jeeves.ucsd.edu.

TABLE 1. Strains and plasmids used

Strain or plasmid	Relevant characteristic(s)	Reference or source
E. coli strains		
BL21	F^- *hsdS* (r_B^- m_B^-) *gal*	48
JM109	*recA1 endA1 gyrA96 thi-1 hsdR17* (r_K^- m_K^+) *supE44 relA1* Δ(*lac-proAB*) (F′ *traD36 proAB lacI*^{q} *ZΔM15*)	58
TG1	[F′ *lacI*^{q} *proA*$^+$ *B*$^+$ *lacZ*ΔM15] *supE44*	6
Plasmids		
pUC18	Cloning vector	55a
pUC19	Cloning vector	55a
pAlter-1	Mutagenesis vector	Promega
pMM40	pKK223-3 expression vector with *lacI*^{q} insertion	25
pGP1-2	p15A replicon carrying the T7 gene *1* RNA polymerase gene	50
pGEX-KG	pGEX-2T with poly(G) linker inserted after thrombin cleavage site	17a
pGEX-KT	pGEX-1 with poly(G) kinker and thrombin cleavage site inserted between *gst* gene and MCS[a]	18
pTD31Δ*Dra*	pBluescript SK(+) carrying P_{parDE} from *Dra*I to *Sau*3AI sites	37
pRR46	Mini-R6K replicon with the P_{parDE}, *parD*, and half of *parE* (to the *Esp*I site)	38
pRR71	3.2-kb stabilization region cloned into pUC19	34a
pRR136-6	pBluescript SK(+) with a 46-bp insertion and *parD* cloned downstream of the vector T7 promoter	37
pAS1	pUC8 with *lacZ*α fused to the 3′ end of the *parD* gene and an intact *parE* gene	38
pAS2	*parE*-(TTG) containing *Eco*RI-*Hin*dIII fragment from pAS1 cloned into same sites of pSelect-1	This work
pAS3	pAS2 mutagenized to insert *Bam*HI site, alter Shine-Dalgarno sequence, and alter start codon to ATG	This work
pAS6	*parE*-(TTG) containing *Eco*RI-*Hin*dIII fragment from pAS1 cloned into same sites of pMM40	This work
pAS11	*parE*-(ATG) containing *Bam*HI-*Hin*dIII fragment from pAS3 cloned into same sites of pGEX-KG	This work
pAS12	*parE*-(ATG) containing *Bam*HI-*Pst*I fragment from pAS11 cloned into same sites of pGEX-KT	This work

[a] MCS, multiple cloning site.

(38). These studies further indicated that ParD and ParE are proteins of a toxin-antitoxin system analogous to those found on plasmids F and R1, with ParE acting as the toxic component. Stabilization of plasmids in *E. coli* by the *parDE* operon has been shown to be accompanied by growth inhibition and filamentation of plasmid-free segregants (38, 46). In addition, plasmids carrying the *parDE* operon can be destabilized by providing ParD in *trans* from a compatible plasmid that is maintained by antibiotic selection (38). While the 9-kDa ParD protein has been shown to regulate the expression of the *parDE* promoter, binding as a dimer, the ParE protein does not appear to contribute to the repression of this promoter (37).

The purpose of this study was to examine further the roles of ParD and ParE as members of a postsegregational killing system and to characterize the interaction of these proteins with each other and with the *parDE* promoter region. We report the purification of ParE′, a 12-kDa cleavage product of a glutathione *S*-transferase (GST)–ParE fusion protein construct. Glutaraldehyde cross-linking studies and a protein binding assay with the GST-ParE fusion protein indicate physical interaction of the ParE′ protein with ParD. ParE′ exists in solution as a dimer and appears to bind to the ParD dimer to form a tetramer. DNA trapping as well as DNase I footprinting and gel retardation experiments indicate that ParE alone does not bind to the promoter, nor does it alter the DNase I footprint of ParD at this sequence. However, the ParE′ protein does bind to the *parDE* promoter region in the presence of the ParD protein. While the ability of ParD to complex to the ParE′ protein is likely to be responsible for preventing the toxin activity of ParE′, the functional significance of the formation of a ParD-ParE-promoter complex is unclear.

MATERIALS AND METHODS

Materials. Restriction enzymes, the Klenow fragment of *E. coli* DNA polymerase, shrimp alkaline phosphatase, T4 DNA ligase, bacteriophage T4 DNA polymerase, T4 polynucleotide kinase, and glutaraldehyde were obtained from commercial suppliers and used according to the manufacturers' instructions. Antibiotics were obtained from Sigma Chemical Company (St. Louis, Mo.). The components of Rich medium are, per liter, as follows: 20 g of tryptone, 10 g of yeast extract, 5 g of sodium chloride (NaCl), 6.8 g of potassium phosphate (monobasic) (KH_2PO_4), and 2 g of glycerol, pH 7.2 (50).

Bacterial strains and plasmids. *E. coli* JM109(pRR46) (58) was used in the construction of pAS12, the overexpression of the fusion protein GST-ParE from pAS12, and the assaying of ParE toxicity. *E. coli* strains were grown in Lennox L broth and, when appropriate, in Rich medium (50). The plasmids used in this study are listed in Table 1. *E. coli* BL21 (48) carrying plasmid pGP1-2 was used for the overexpression of ParD from plasmid pRR136-6. *E. coli* TG1 (6) was also used for plasmid constructions. Plasmids were selected with 250 μg of penicillin per ml or 50 μg of kanamycin per ml when necessary.

DNA manipulations were performed as previously described (41). The construction of pAS6 required that the *Eco*RI-*Hin*dIII fragment of pAS1 containing *parE* be cloned into the same restriction sites of pMM40 (25). This placed *parE* downstream of the IPTG (isopropyl-β-D-thiogalactopyranoside)-inducible *tac* promoter. The construction of pAS12 (from pAS1) was performed by initially cloning the *parE*-containing *Eco*RI-*Hin*dIII fragment of pAS1 into the same sites of pAlter-1 (Promega, Madison, Wis.) to produce pAS2. Plasmid pAS2 was then altered to produce pAS3, using the Altered Sites protocol of Promega and an oligonucleotide with the sequence 5′-GAT CTG TCA GCG AGG ATC CCG CAT GAC GGC CTA CA-3′. These alterations improved the Shine-Dalgarno sequence of *parE*, introduced a new *Bam*HI site, and changed the start codon from TTG [*parE*-(TTG)] to ATG [*parE*-(ATG)]. The sequence of the mutagenized region was verified by DNA sequencing. Plasmid pAS11 was constructed by inserting the *Bam*HI-*Hin*dIII fragment of pAS3, containing *parE*-(ATG), into the same restriction sites of pGEX-KG. The *Bam*HI-*Pst*I fragment of pAS11 containing *parE*-(ATG) was inserted into the same restriction sites of pGEX-KT to produce pAS12. In this construct, the *tac* promoter drives a fusion protein consisting of GST followed by a kinker region of five glycine residues, a thrombin cleavage site, and *parE*-(ATG) cloned in frame. The fusion protein can be cleaved with thrombin, generating a ParE derivative, designated ParE′, which contains three extra amino acids (Gly, Ser, and Arg) prior to the first methionine.

ParE toxicity assay. Plasmids pAS6 and pAS12 were introduced by transformation into *E. coli* JM109 and JM109(pRR46) by a standard transformation procedure (41). Transformation mixes were grown at 37°C on Rich medium plates containing either penicillin or penicillin and kanamycin, at concentrations of 250 and 150 μg/ml, respectively, and, when necessary, 120 μg of IPTG per ml.

Purification of GST-ParE. Purification of the GST-ParE protein was performed essentially as previously described (18). JM109(pRR46, pAS12) was grown overnight at 37°C in 30 ml of Rich medium with penicillin and kanamycin but without shaking. The culture was then incubated with shaking for 30 min and transferred to 750 ml of Rich medium containing antibiotics. At an optical density at 600 nm of 2.5, IPTG was added to a final concentration of 0.4 mM, and incubation was continued for an additional 2 h. Cells were harvested and washed once in 40 ml of 20 mM sodium phosphate (pH 7.6), and the pellet was resuspended in PBST buffer (20 mM potassium phosphate, 150 mM NaCl, 1% Triton X-100, and 0.1% β-mercaptoethanol [pH 7.6]). Approximately 3 g of cells was lysed by sonication. After centrifugation, the supernatant was mixed with a 4-ml bed volume of glutathione-agarose beads (Sigma Chemical Co.) by tumbling for

30 to 40 min at 4°C. After three washes with PBST and three washes with thrombin cleavage buffer (TCB) (50 mM Tris-HCl, 150 mM NaCl, 2.5 mM $CaCl_2$, and 0.1% β-mercaptoethanol [pH 8.0]), the GST-ParE protein was eluted from the glutathione-agarose matrix with 5 ml of TCB containing 10 mM reduced glutathione (Sigma). An additional amount of 5 mM glutathione was then added to the beads, and the mixture was transferred to a column (Pharmacia) and eluted by gravity flow. Eluents were combined, filtered (Acrodisc, 0.2 μm; Gelman Sciences), and dialyzed for 3 h with two changes into 500 ml of buffer A (20 mM HEPES [*N*-2-hydroxyethylpiperazine-*N*′-2-ethanesulfonic acid] [pH 8.0], 1 mM EDTA, 1 mM dithiothreitol [DTT]) (33) plus 50 mM KCl. After dialysis, centrifugation (10 min, 6,000 × *g*) followed by refiltration to remove any precipitated protein was carried out. Since GST-ParE often precipitated when stored overnight at 4°C, the protein was loaded immediately onto a Mono-S fast protein liquid chromatography (FPLC) column (HR 5/5; Pharmacia) and eluted with a linear 50 to 550 mM KCl gradient in buffer A. Upon collection of the peak fractions (at approximately 350 mM KCl), 1 ml of buffer A and 50 mM KCl were added to each of the 0.5-ml peak fractions to prevent precipitation of the protein. The fractions were immediately dialyzed (3 h, two changes, 4°C) against TCB and stored at 4°C. Generally, approximately 0.6 mg of purified GST-ParE was recovered with this procedure. In the purification of the GST protein, JM109 (pGEX-KT) was used for preparation of the lysate as described above with omission of the FLPC purification step.

Purification of ParE′. ParE′ was purified as described above up to the elution step, in which ParE′ was eluted from the glutathione matrix with the addition of 13.5 U of thrombin (Bovine Plasma; Sigma) at 25°C. After centrifugation of the matrix and collection of the eluent, the incubation step was repeated, and the beads were poured into a column and then allowed to elute by gravity at 25°C. The various eluents (9.6 mg of total protein from 6.92 g of cells) were mixed, filtered (Acrodisc, 0.2 μm; Gelman Sciences), and dialyzed against buffer D (50 mM HEPES [pH 8.0], 50 mM KCl, 5 mM $MgCl_2$, 1 mM DTT). ParE′ was further purified by FPLC. The peak ParE′ fraction was eluted from the FPLC column at approximately 390 mM KCl. The total amount of ParE′ recovered was approximately 1.3 mg. Protein samples recovered from the purification steps were analyzed by sodium dodecyl sulfate-polyacrylamide gel electrophoresis (SDS-PAGE) (27, 43) and visualized by either Coomassie brilliant blue R (Sigma), silver staining (30), or Western blotting (immunoblotting) (26). Protein concentrations were determined by the Bio-Rad protein assay (Bio-Rad Laboratories, Richmond, Calif.) with the protocol supplied.

ParD trapping on GST-ParE. ^{35}S-labeled ParD, labeled and purified as described previously (37), was obtained from R. C. Roberts. Cultures of JM109(pRR46, pAS12) and JM109(pRR46, pGEX-KT) were grown and induced as described above to obtain a GST-ParE extract and a control extract, respectively. Cell pellets were resuspended in 3 ml of PBST and lysed by sonication. Lysates were centrifuged (20 min, 10,000 × *g*, 4°C), and the supernatant was mixed with 0.75 ml of glutathione-agarose beads for 30 to 40 min at 4°C. A solution consisting of 250 μl of PBST containing 100 mg of ParD with a ratio of labeled to unlabeled ParD of 0.01:1 was then added to each sample. After incubation with stirring for 30 min at 4°C, the beads were washed four times in 6 ml of PBST and three times in 6 ml of TCB. Bound GST-ParE was eluted by the addition of TCB containing 5 mM glutathione. Samples were incubated at 4°C with gentle mixing and then centrifuged, and the supernatants were collected. The beads were washed five times in 1 ml of TCB with 5 mM glutathione. The amount of labeled ParD protein in the supernatants was measured by scintillation counting.

ParD and ParE′ cross-linking. Three protein solutions were prepared in cross-linking buffer (50 mM HEPES [pH 8.0], 50 mM KCl, 5 mM $MgCl_2$); one contained ParD, another contained ParE′, and the third contained both ParD and ParE′. The solutions were mixed and incubated at 0°C for 15 min. Portions (18 μl) of each solution (2 μg of each protein) were incubated with glutaraldehyde at concentrations of 0, 0.1, and 0.5%, respectively. Each protein was at a final concentration of 0.1 μg/μl. Cross-linking reaction mixtures were incubated at 15°C for 5 min, and the reactions were stopped by adding 8 μl of stop solution (0.44 M Tris [pH 6.8], 8% SDS, 40% glycerol, 80 mM DTT, 0.004% bromophenol blue). Reaction products were analyzed by low-molecular-weight resolving PAGE (43) and visualized by silver staining (30).

DNA trapping by the GST-ParE–ParD complex. The ability of ParD to bind ParE′ and the *parDE* promoter was determined as previously described with modifications (44, 45). The gel-purified DNA fragments used for this study were obtained by digestion of plasmid pRR71 with *Bam*HI and *Eco*RI. The 3.2-kb *par* region is on a single fragment after digestion. The 3.2-kb fragment was purified and then digested with *Rsa*I to yield seven blunt-ended fragments, the largest of which (936 bp) contains the *parDE* promoter region. The 5′ ends of the fragments were dephosphorylated with shrimp alkaline phosphatase, and the fragments were radiolabeled with [γ-^{32}P]ATP by a forward reaction kinase protocol for blunt-ended fragments (41).

Six samples consisting of a 100-μl bed volume of glutathione-agarose equilibrated with PBST and 350 μl of sonicated JM109 cell extract were prepared. The extract was obtained by resuspending 1.5 mg of pelleted JM109 cells in 3.5 ml of PBST, lysing by sonication, and centrifuging for 20 min at 10,000 × *g* to remove cellular debris. Two of the samples contained no added protein, two of the samples were amended with 10 μg of GST, and the remaining two were amended with 10 μg of GST-ParE. Each sample was incubated at 4°C for 30 to 40 min with mixing; this was followed by the addition of 5 μg of ParD to one of each of the three sets of tubes and incubation at 4°C for 30 to 40 min with mixing. Unbound proteins in each sample were removed by three washes in 1 ml of PBST and one wash in DNA binding buffer (45) (25 mM HEPES [pH 8.0], 100 mM KCl, 20% glycerol, 0.1% Nonidet P-40, 10 μM $ZnSO_4$, 5 mM DTT), and then 350 μl of DNA binding buffer and 1 μg of *Alu*I-digested pUC18 (58) were added to each tube. After incubation for 15 min at 4°C, 4 ng of radiolabeled, *Rsa*I-digested 3.2-kb region was added to each sample. The tubes were incubated at 25°C for 20 min, after which the unbound DNA was removed by washing the beads three times in DNA binding buffer. One hundred fifty microliters of DNA binding buffer was then added to the beads, and phenol-chloroform extraction was performed to release the DNA fragments from the matrix. The DNA sample was then ethanol precipitated after the addition of 3 μg of glycogen as a carrier, resuspended, and analyzed by 5% PAGE (41).

DNA-bound protein exclusion. The abilities of ParD and ParE to bind to the promoter region were examined by using a sizing column exclusion protocol as previously described (57) with the following modifications. The DNA fragments used for this study were obtained by cleaving pTD31 (8) with *Pst*I and *Hin*dIII, which produced a 548-bp fragment of the 3.2-kb region containing the *parDE* promoter region. An aliquot of the DNA was end labeled with [α-^{32}P]dATP by treatment with Klenow fragment to fill in the *Pst*I cleavage site (41). The concentrations of ParD and ParE′ were 5 and 4 μg per reaction mixture, respectively. The concentrations of nonlabeled and labeled DNA were 4 μg and 4 ng per reaction mixture, respectively. Proteins were mixed in a final volume of 25 μl of DNA binding buffer and incubated at 25°C for 15 min. DNA in 25 μl of DNA binding buffer was then added, and the mixtures were incubated at 4°C for 15 min.

Columns (0.8 ml) prepared in 1-ml sterile syringes containing Sepharose CL-6B (Pharmacia) were washed before use with 2 volumes of sterile water and 2 volumes of DNA binding buffer. Binding reaction mixtures were added to each column and eluted by gravity in DNA binding buffer at 25°C. Fractions of 2 to 4 drops (approximately 34 to 68 μl) were collected. The fractions with the highest radioactivity were pooled and analyzed by PAGE on a low-molecular-weight protein resolving gel and visualized by silver staining. In the case of samples of ParD and ParE′ without DNA, the peaks could not be identified by monitoring radioactivity; therefore, peak fractions were assumed to be the same as in the case of ParE′ plus DNA.

Gel mobility shift analysis. The effect of ParE′ on the binding of ParD to P_{parDE} was examined by using a modification of gel retardation protocols described previously (21, 33). The radiolabeled DNA fragments used for this study were the same as used for the DNA trapping study described above. ParD and ParE′ were diluted to the desired concentration in TBE (41) with 1 μg of poly[d(I-C)] in a final volume of 10 μl. Proteins were mixed and incubated at 0°C for 10 min, and then 1 ng of labeled DNA fragments in 10 μl of TBE was added. After incubation at 25°C for 20 min, 2 μl of a 25% Ficoll 400 solution was added to each reaction mixture. The samples were then analyzed by 5% PAGE as described previously (41).

DNase I footprinting analysis of P_{parDE}. The DNA probes used for DNase I footprinting were prepared and used as described previously (37, 38). ParE′ and ParD were initially mixed in a final volume of 10 μl of footprinting buffer (50 mM HEPES [pH 7.6], 10 mM $MgCl_2$, 100 mM KCl, 1 mM DTT, 0.1 mg of bovine serum albumin per ml). ParD was held constant at 400 ng per reaction mixture, while ParE′ amounts ranged from 0 to 1,600 ng per reaction mixture. After incubation at 25°C for 10 min followed by the addition of 0.25 ng of probe in 10 μl of probe solution {1× footprinting buffer, 0.2% Nonidet P-40, 0.5 μg of poly[d(I-C)]}, the samples were incubated for 20 min at 25°C. Two microliters of DNase solution (1× footprinting buffer, 25 mM $CaCl_2$, 1 ng of DNase I per μl) was then added, and the mixtures were incubated at 25°C for 30 s. The reactions were then stopped by the addition of 2 μl of stop buffer (200 mM Tris [pH 7.4], 100 mM EDTA, 2% SDS) and chilling on ice. The reaction mixtures were then deproteinized and analyzed by gel electrophoresis as previously described (41).

RESULTS

Purification of GST-ParE and ParE′. To facilitate the purification of ParE, several expression vectors were constructed. Plasmid pAS6 (Fig. 1A) is a pBR322-based vector carrying a *parE*-containing fragment derived from pAS1 (38) with *parE* under the control of the *tac* promoter. This construct did not give high levels of expression of ParE, and therefore, a GST-ParE fusion construct, pAS12 (Fig. 1A), in which *parE*-(ATG) was inserted in frame at the C-terminal end of the GST gene on the pBR322-based vector pGEX-KT (18), was made. The resulting GST-ParE fusion protein includes a thrombin cleavage site (7) downstream from a kinker region of five glycine residues which maximizes access of thrombin to the cleavage site (Fig. 1B). Thrombin cleavage generates a ParE derivative with three additional amino acids, glycine, arginine, and serine,

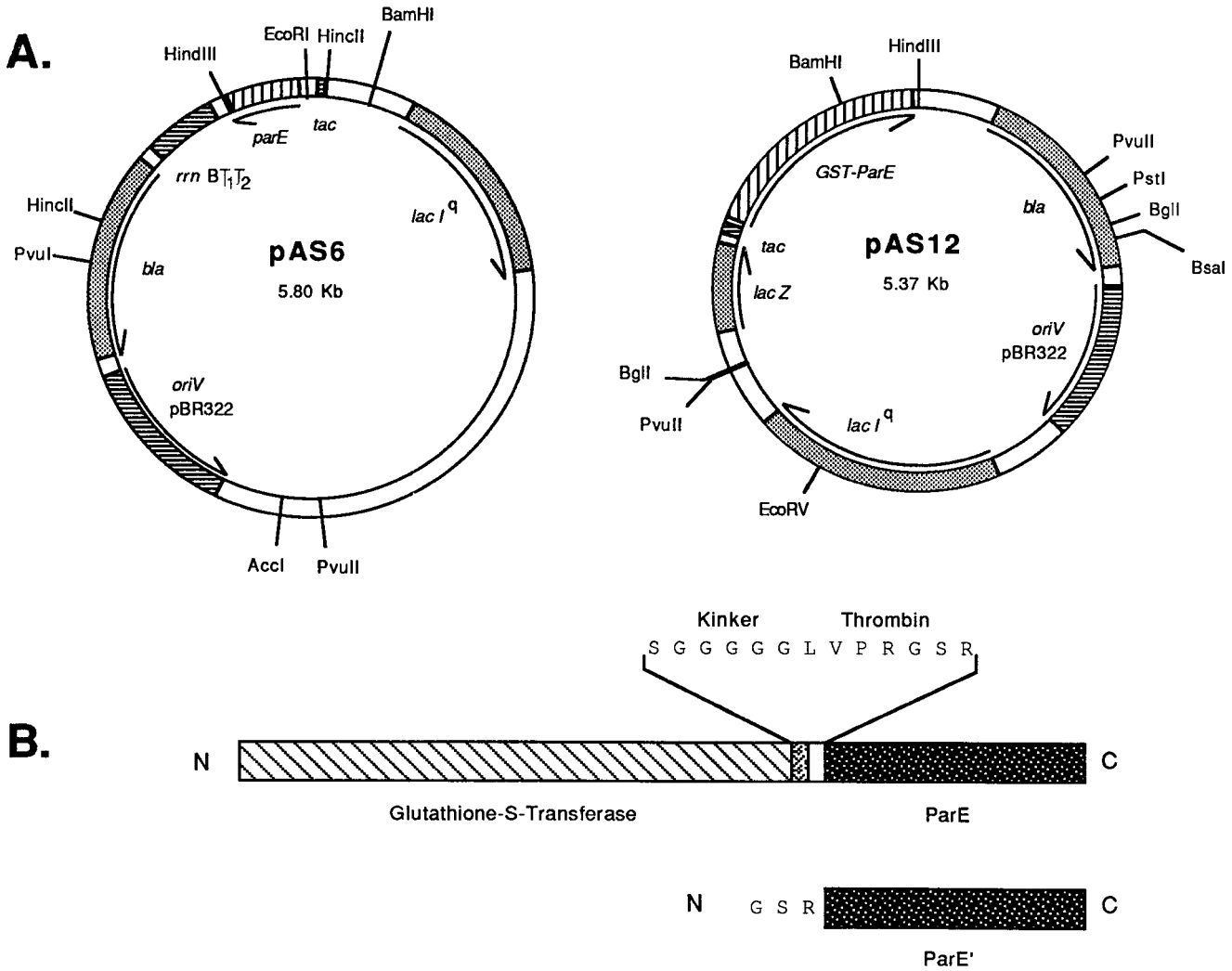

FIG. 1. (A) Plasmids used to express the ParE and GST-ParE proteins. Construction is described in Materials and Methods. *oriV* is the origin of vegetative replication, *bla* is the β-lactamase gene encoding penicillin resistance. *lacI*^{q} encodes the repressor which regulates the *tac* promoter, and *rrnB*T_1T_2 is the transcriptional terminator from the *E. coli rrnB* operon. (B) Cleavage of GST-ParE with thrombin at the indicated thrombin cleavage site produces ParE′, a ParE derivative with three extra amino acids and containing methionine in place of leucine at the normal N-terminal position of ParE.

prior to the first methionine. This derivative, designated ParE′, was used in all experiments requiring purified ParE. Upon induction with IPTG, strains carrying pAS12 express GST-ParE at high levels.

In the construction of pAS12, the GST-ParE vector could not be established within a bacterial host without the provision of ParD in *trans*, because uninduced levels of GST-ParE were lethal to the host. For this reason, ParE-expressing plasmids were transformed into *E. coli* JM109 containing pRR46, an R6K-based replicon carrying *parD* and approximately one-half of *parE* under the control of the *parDE* promoter (38). Plasmid pRR46 expresses ParD and an inactive, truncated ParE protein.

To further characterize the toxic activity of ParE in vivo, an assay in which *E. coli* JM109 or JM109(pRR46) was transformed with pUC19, pAS6, or pAS12 was done (Table 2). Transformed cells were then plated on agar with or without IPTG. In the case of *E. coli* JM109, only uninduced transformants containing pAS6 were obtained. Induced pAS6 transformants and pAS12 transformants, with or without induction, were not obtained, presumably because of the cell-killing effects of either ParE or GST-ParE. When ParD was provided in *trans*, transformants of *E. coli* JM109(pRR46) were obtained in all assays, with the exception of cells transformed with pAS12 and induced. These results suggested a correlation between the level of expression of ParE and cell killing. Without the ParD

TABLE 2. Transformation efficiency with ParE-expressing plasmids

Plasmid	Transformants/μg of plasmid DNA:			
	Without IPTG		With IPTG	
	JM109	JM109(pRR46)	JM109	JM109(pRR46)
pUC19	5.0×10^4	8.0×10^4	ND[a]	ND
pAS6	2.0×10^4	2.8×10^4	0[b]	8.5×10^4
pAS12	0	9.9×10^3	0	0

[a] ND, not determined.
[b] 0, no transformants were obtained after plating of approximately 10^8 cells made competent and transformed with 100 ng of DNA.

antitoxin provided in *trans*, all but very low levels of ParE expression prevented cell growth, while JM109 carrying ParD survived the expression of ParE except at very high levels. The frequency of pUC19 transformation was observed in separate experiments to be approximately the same after plating on plates with or without IPTG (data not shown). These results are consistent with previous reports which indicated that ParE is the toxic component of the killing system while ParD is the antitoxin (23, 38).

The protein purification procedures employed in our studies yielded GST-ParE which was approximately 95% pure after FPLC purification. Thrombin cleavage of GST-ParE while bound to the glutathione matrix yields ParE′, which was further purified by FPLC. FPLC purification of ParE′ yielded two protein peaks, a smaller peak eluting at about 270 mM KCl and a second, larger peak eluting at about 390 mM KCl. Analysis by PAGE and visualization by silver staining or Western blotting demonstrated that the first and smaller peak consisted of roughly equal amounts of ParD and ParE′ (data not shown). Peak II consisted of greater than 95% pure ParE′. This suggests a strong physical interaction between the two proteins, resulting in the formation of a stable complex under different buffer conditions. Multiple peaks were also observed during FPLC purification of GST-ParE. In this case, ParD again copurified with GST-ParE as a relatively small and early peak in addition to being present within the shoulder of the major GST-ParE peak.

ParD-ParE complex formation. Since it is likely that ParD protects host cells from the toxic effects of ParE by complexing with ParE, the physical interaction between the two proteins was further investigated. Initial experiments to analyze the ability of ParD to complex with ParE involved determining whether ^{35}S-labeled ParD bound to a glutathione-agarose affinity matrix to which GST-ParE had been bound. ^{35}S-labeled ParD was added to the glutathione matrix containing bound GST-ParE, and unbound protein was removed by several washes. GST-ParE was then eluted by the addition of glutathione, and the eluents and the amount of ^{35}S-labeled ParD were determined by scintillation counting. Trials were also done in which GST was bound to the matrix instead of GST-ParE to control for nonspecific binding of ParD to the matrix or to the GST region of the GST-ParE protein. The percentage of labeled ParD remaining on the glutathione matrix after subsequent washes and elutions with glutathione is shown in Fig. 2. In control trials in which GST was bound to the matrix, 48% of labeled ParD remained bound to the matrix after several washes. Little additional ParD was removed with the elution of GST by the addition of glutathione. When GST-ParE was bound to the matrix, 98% of the added ParD remained after unbound protein was removed. With elution of the GST-ParE, 59% of bound ParD was removed from the glutathione matrix. These results suggest that ParD binds to the ParE protein.

The nature of the ParD-ParE interaction was investigated further by covalent cross-linking of ParD-ParE′ mixtures with glutaraldehyde. The ParD and ParE′ proteins were incubated either separately or together, a glutaraldehyde solution was added, and PAGE analysis was performed. In the reactions with ParD only (Fig. 3, lanes 1 to 3), bands corresponding to a dimeric form of ParD could be observed in the lanes with added glutaraldehyde (Fig. 3, lanes 2 and 3). This is consistent with previous results suggesting that ParD binds to P_{parDE} as a dimer (37). A dimeric band also appeared in the reactions with ParE′ alone after cross-linking (Fig. 3, lanes 5 and 6), suggesting that ParE also exists as a dimer in solution. No higher multimeric forms could be observed with either ParD alone or

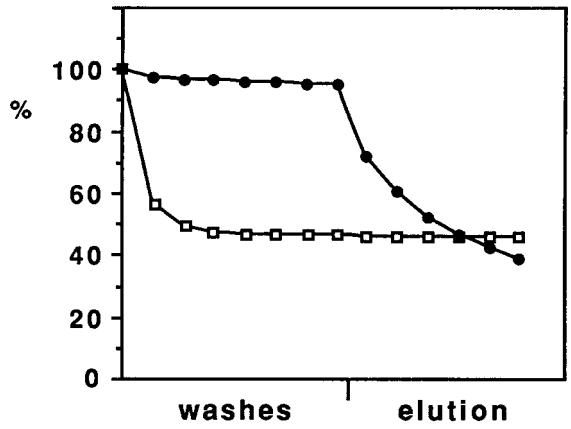

FIG. 2. Binding of ParD to GST-ParE on a glutathione-agarose affinity matrix. The graph indicates the percentage of retained ^{35}S-labeled ParD bound to GST (□) or GST-ParE (●) after a series of washes followed by elutions with glutathione.

ParE′ alone under the assay conditions employed. When the two proteins were mixed together and cross-linked (Fig. 3, lanes 8 and 9), several extra bands were observed. At 0.1% glutaraldehyde, a band of intermediate size between the ParD and ParE′ dimer bands appeared. The position of this band is consistent with the formation of a heterodimeric form. In addition, a higher band was observed, approximately at the position of a trimer. At 0.5% glutaraldehyde, a still higher band appeared at a position corresponding to an approximately 44-kDa protein, suggesting the formation of a tetramer. These

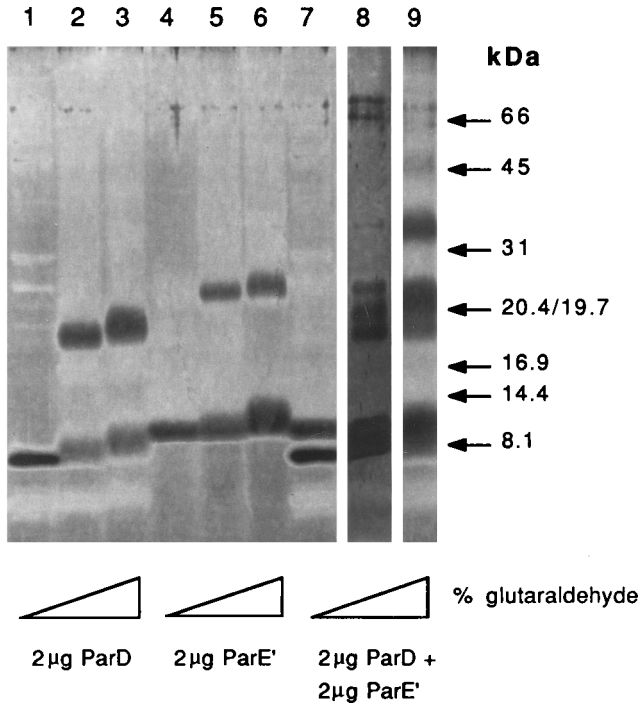

FIG. 3. ParD and ParE′ cross-linking with glutaraldehyde. Lanes 1 to 3 contain 2 μg of ParD, lanes 4 to 6 contain 2 μg of ParE′, and lanes 7 to 9 contain 2 μg each of ParD and ParE′. Glutaraldehyde was used at final concentrations of 0% (lanes 1, 4, and 7), 0.1% (lanes 2, 5, and 8), and 0.5% (lanes 3, 6, and 9). The positions of standard proteins are shown on the right.

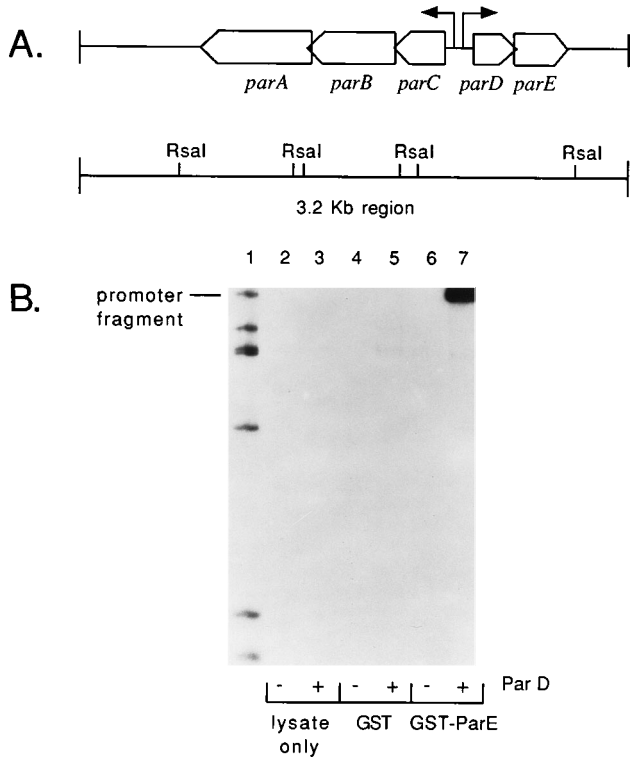

FIG. 4. (A) Physical map of the 3.2-kb RK2 stabilization region. On the line below the map, *Rsa*I cleavage sites that produce fragments used in DNA trapping and gel mobility shift assays are shown. (B) DNA recovered from glutathione-agarose charged with *E. coli* lysate only (lanes 2 and 3), lysate with 10 μg of GST added (lanes 4 and 5), and lysate with 10 μg of GST-ParE added (lanes 6 and 7). Five micrograms of ParD was also added to the mixtures represented by lanes 3, 5, and 7. Lane 1 contains DNA from *Rsa*I cleavage of the 3.2-kb region for reference.

results seem to indicate that both ParD and ParE exist as dimers in solution. Furthermore, the data suggested that dimers of these proteins associate to form a heterotetrameric complex. It is likely that the trimeric and dimeric forms (Fig. 3, lane 9) are a result of incomplete cross-linking of a tetrameric form consisting of dimers of ParD and ParE. However, the possibility that the ParD-ParE complex exists in either trimeric, heterodimeric, or higher multimer forms cannot be ruled out at this time.

Binding of the P_{parDE} DNA fragment by the ParD-ParE complex. Previous results have shown that the dimer form of ParD has an autoregulatory role, binding to a 48-bp sequence within the *parDE* promoter region to repress transcription of *parDE* (10, 37). Our results suggest that the ParD and ParE proteins associate to form a tetramer in solution. It is therefore possible that a ParD-ParE complex also binds at the promoter and perhaps elsewhere within the 3.2-kb stabilization region of RK2 that includes the two operons *parDE* and *parCBA*. To investigate this, the GST-ParE fusion protein was used to determine if a GST-ParE–ParD complex binds to P_{parDE} DNA. Purified GST-ParE was added to a whole-cell extract prepared from *E. coli* JM109, and the mixture was added to a glutathione matrix. After an incubation period to allow binding, purified ParD was added. Radiolabeled DNA fragments representing the entire 3.2-kb RK2 stabilization region were then added to the GST-ParE–ParD-charged matrix. These fragments were generated by cleaving purified 3.2-kb DNA with *Rsa*I to produce seven fragments of various lengths (Fig. 4A). The *parDE* promoter is located on the largest (936-bp) fragment. All seven fragments were tested to determine if any other region of the 3.2-kb fragment would be bound by the ParD–GST-ParE complex. After removal of unbound DNA fragments by several washes, the glutathione-agarose matrix was subjected to phenol-chloroform extraction to denature protein and free trapped DNA. Recovered DNA was analyzed by PAGE. Control experiments were done in which no protein or only GST protein was added to the glutathione-agarose matrix instead of GST-ParE. Another set of tests of binding to the GST-ParE-bound matrix were carried out without the addition of ParD. No DNA fragment was trapped unless both GST-ParE and ParD were present (Fig. 4B, lane 7). GST-ParE alone did not appear to trap any fragment, suggesting that ParE alone does not bind to the 3.2-kb region at any location (assuming that *Rsa*I cleavage does not inactivate a ParE binding sequence). Since GST-ParE was required for ParD binding to the glutathione-agarose matrix in this system, the trapping of the promoter fragment on the matrix suggests that ParD binds to both the promoter region and ParE simultaneously. Furthermore, since the ParD–GST-ParE complex bound only to the 936-bp P_{parDE}-containing fragment, it would seem that the ParD-ParE complex binds only to the promoter and not to any other sequence within the 3.2-kb region.

To further test the hypothesis that both ParD and ParE bind to the *parDE* promoter region as a complex, a DNA exclusion experiment utilizing Sepharose CL-6B (Pharmacia) was done. This matrix has a globular protein molecular mass range of 10 to 4×10^3 kDa and excludes DNA fragments larger than 194 bp. In this experiment, ParD and ParE′ were mixed and then added to a 548-bp fragment containing the *parDE* promoter. After incubation to allow association of protein with DNA, the reaction mixture was run through the matrix. The 548-bp DNA fragment was excluded from the column and eluted in the void volume. Any proteins that were bound to the DNA should also be present in the void volume. Unbound ParD, ParE′, and multimeric forms of these proteins are fully included in the sizing column and thus were eluted in later fractions. A molar ratio of ParE′ to ParD of approximately 0.8:1 was chosen to avoid titration of ParD from the promoter region, which is observed at very high ParE′/ParD ratios in gel mobility shift and DNase I footprinting assays (see below). The molar ratio of ParD to P_{parDE} was 25:1. A radiolabeled 548-bp fragment was added to monitor progress of the excluded DNA fragments through the column. Fractions from the column were also analyzed by PAGE and silver staining. Control experiments were carried out in which both ParD and ParE′, but no DNA, was used and in which ParE′ alone was incubated with DNA. In the cases of ParD plus ParE′ but no DNA and ParE′ plus DNA (Fig. 5, lanes 3 and 4, respectively), no protein could be detected in the void volume, while in the case of ParD plus ParE′ and DNA, both ParD and ParE′, in approximately equivalent amounts, were observed in the void volume (Fig. 5, lane 5). Thus, the ParE′ protein binds to a DNA fragment carrying the promoter region but only in the presence of the ParD protein. This supports the conclusion of the DNA trapping experiment, namely, that ParE′ alone does not appear to bind the promoter region but must be complexed with ParD for binding.

Effect of ParE-ParD complex formation on ParD binding to the *parDE* promoter. Previous in vivo studies indicated that ParD alone is necessary for full transcriptional repression of the *parDE* operon (37). Evidence presented in this study indicating that a complex of ParD and ParE binds at P_{parDE} suggests that ParE might have some role at the promoter region, as shown for the toxic proteins of the *ccd* and *parD* killing

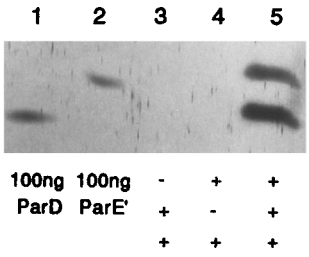

FIG. 5. DNA exclusion experiment, showing protein excluded from a Sepharose CL-6B column. Lanes 1 and 2 contain 100 ng of purified ParD and ParE′, respectively. Lanes 3, 4, and 5 represent proteins found in the void volume when the ParE′ protein is present with or without the ParD protein and in the presence or absence of DNA containing the *parDE* operon. In each case, a radiolabeled promoter fragment was used to determine the peak DNA elution fractions. Two fractions from each peak of DNA, or comparable fractions if DNA was not present, were pooled and analyzed by PAGE.

systems of F and R1, respectively (9, 39, 40). Two approaches were used to determine the effect of ParE′ on the binding of ParD to the *parDE* promoter region. The first was a gel mobility assay using the same DNA fragments as used in the DNA trapping experiment (described above). Purified ParD alone or preincubated with various concentrations of ParE′ was added to *Rsa*I-cut radiolabeled fragments of DNA. The ParD concentration was held constant (1 μg per sample), while the amount of ParE′ varied from 100 to 2,000 ng per sample. Additional samples with 2 μg of ParD alone, 2 μg of ParE′ alone, and no protein were included. On the basis of DNA retardation, ParD bound to the 936-bp promoter-bearing fragment but not to any of the other fragments (Fig. 6, lane 7), indicating that the promoter region is most likely the sole binding site within the 3.2-kb region (assuming again that *Rsa*I cleavage does not inactivate a ParD binding site). ParE′ alone did not appear in this assay to bind to any fragment (Fig. 6, lane 8). There was, however, a ParE′ concentration-dependent effect on ParD binding to the promoter region. As the ParE′ protein concentration was increased, the shifted band gradually became more retarded (Fig. 6, lanes 1 to 5). At 2,000 ng of ParE′, when the molar ratio of ParE′ to ParD was approximately 2:1, the 936-bp band was less retarded than in the absence of ParE′ (Fig. 6, lane 6). The position and diffuse appearance of the promoter fragment in lane 6 of Fig. 6 are similar to those observed when low concentrations of ParD are used (37).

To further examine the effect of the ParE′ protein on ParD-P_{parDE} binding, DNase I footprinting assays were carried out to determine whether the footprint of ParD is altered by the presence of ParE′. In these studies, the concentration of ParE′ was varied from 0 to 1,600 ng per reaction mixture, while the concentration of ParD was held constant at 400 ng per reaction mixture. In the case of ParE′ only (Fig. 7, lanes 9 and 18), no DNase I protection was observed. This is consistent with the DNA trapping and gel mobility shift assays that showed that ParE′ does not bind directly to the *parDE* promoter. Furthermore, it was observed that ParE′ did not change the footprint of ParD at the *parDE* promoter (Fig. 7, lanes 2 to 6 and 11 to 15) unless very high concentrations of ParE′ (Fig. 7, lanes 7, 8, 16, and 17) were used. At ParE′/ParD ratios of 2:1 and higher, a loss of protection was observed. In view of the DNA trapping and gel retardation studies which demonstrate the binding of a ParD-ParE′ complex at the promoter region, it is surprising that ParE′ does not change the footprint of ParD at the promoter region.

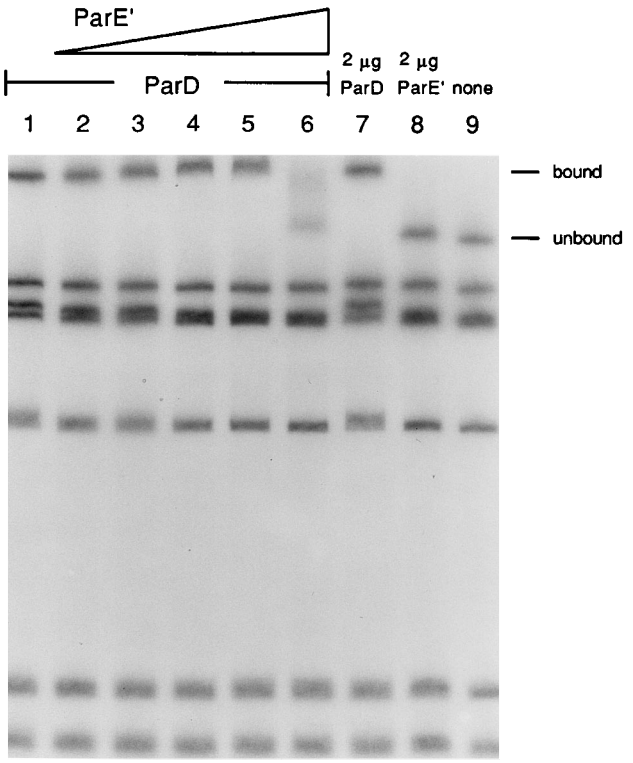

FIG. 6. Gel mobility shift assay. The DNA fragments used were the same as in the DNA trapping assay, and 1 ng of labeled DNA was used in each reaction. In lanes 1 to 6, ParD was held constant at 1,000 ng of protein, while ParE′ was added at 0, 100, 200, 500, 1,000, and 2,000 ng, respectively. In lanes 7 and 8, binding reactions were done with 2,000 ng of ParD or 2,000 ng of ParE′ alone, respectively. Lane 9 contains no protein. The positions of bound and unbound promoter fragments are shown.

DISCUSSION

Previous work has demonstrated that the 0.7-kb region, a segment of the 3.2-kb region which encodes the entire *parDE* operon, stabilizes plasmids via a growth inhibition or cell-killing mechanism (38, 46). These results suggested that ParE is a toxin, while ParD is an antitoxin protein that neutralizes the activity of ParE. The *E. coli* transformation assay carried out in this study supports this conclusion. In the absence of ParD, only a plasmid which expressed very low levels of ParE was able to be established in *E. coli* JM109. When ParD was provided in *trans*, all ParE-expressing plasmids could be established, with the exception of a plasmid construct that expresses very high levels of GST-ParE, a GST fusion derivative of ParE. It is of interest that the GST-ParE fusion protein retains the toxic activity of the ParE protein. It is also, therefore, very likely that ParE′ retains the toxic activity of ParE in addition to its ability to form a complex with ParD.

ParE′ and GST-ParE were initially purified from *E. coli* JM109 carrying plasmids pAS12 and pRR46, which express GST-ParE and ParD, respectively. The presence of ParD was required to protect the cells from the toxic effects of the fusion protein. Its presence, however, complicated purification of GST-ParE and ParE′, since it copurified with both proteins. Purification with FPLC and a cation-exchange column took advantage of the positive charge of ParE, which has a predicted pI of 11.2. ParD remained complexed with ParE′ and GST-ParE during FPLC purification, but the ParD complexes present eluted separately from ParE′ or GST-ParE alone, re-

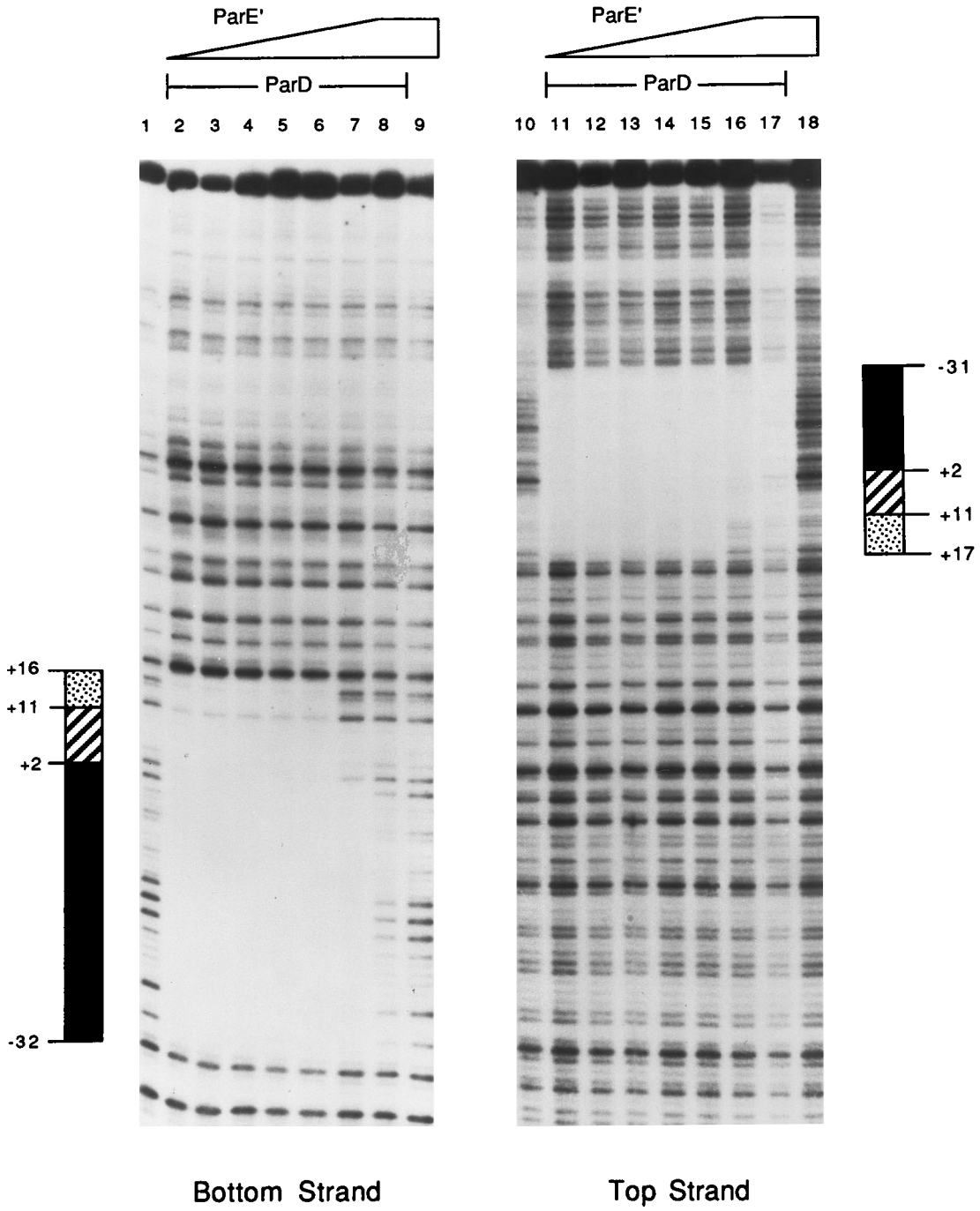

FIG. 7. DNase I footprinting of the *parDE* promoter region. Binding to each of the two strands (lanes 1 to 9 and 10 to 18) was examined. The reaction mixtures in lanes 1 and 10 included no protein. In lanes 2 to 8 and 11 to 17, ParD concentrations were held constant at 400 ng per 20-μl reaction mixture, while ParE′ was added at 0, 50, 100, 200, 400, 800, and 1,600 ng per reaction mixture, respectively. The reaction mixtures in lanes 9 and 18 included 1,600 ng of ParE′ and no ParD. One nanogram of probe DNA was used in each binding reaction mixture.

sulting in a greater than 95% purity of ParE′ as judged by PAGE analysis and silver staining. The GST-ParE protein was obtained in a somewhat less pure form than ParE′.

The formation of a complex between ParD and ParE was initially suggested by ParD trapping experiments in which ParD complexed with GST-ParE bound to the glutathione-agarose matrix. The ParD-ParE complex was further characterized by glutaraldehyde cross-linking. The cross-linking studies are consistent with earlier experiments which suggested that ParD binds to the *parDE* promoter as a dimer (37). ParD and ParE′ are shown in this work to each exist largely in the dimeric form in solution. Higher multimeric forms were not observed for either the ParD or ParE′ protein alone. When these proteins are present together, cross-linking results suggest the presence of higher multimer forms. Bands running at the positions of tetramer, trimer, and heterodimer were ob-

served, suggesting the formation of a tetrameric complex involving the dimer forms of ParD and ParE. These results support the model that the antitoxin activity of ParD involves the formation of a complex with ParE which prevents the expression of ParE toxin activity.

The likelihood that ParE′ complexes with the ParD protein raised the possibility that ParE influences the binding of the ParD protein to the *parDE* promoter. DNA trapping and protein exclusion experiments suggest that both proteins bind to the promoter, presumably as a complex. These same analyses indicate that the ParD-ParE′ complex does not bind to other regions of the 3.2-kb stabilization region.

It has been shown that ParE is not required for full autorepression of P_{parDE} by ParD (8). This is in contrast to the functionally homologous *ccd* and *parD* loci of plasmids F and R1, respectively. In these systems, both proteins of the postsegregational cell-killing system are required for full repression of their expression (9, 39, 40). Gel mobility and DNase I footprinting assays were carried out to examine the possibility that the ParE protein is active at the *parDE* promoter. Previous studies showed that ParD binds as a dimer to a 48-bp region of the promoter (37). In the current study, ParE′ alone does not bind to the promoter region, but, in combination with ParD, the DNA fragment carrying the promoter region is gradually more shifted in gel retardation as the ParE′ concentration increases. It is possible that this further retardation of the promoter fragment is a function of effect of ParE′ on the migration of ParD and occurs independently of DNA. DNase I footprinting assays showed no change in the footprint of ParD at the promoter region as the ParE′ concentration was gradually increased up to a molar ratio of approximately 1:1. However, at higher concentrations of ParE′, changes in the footprint did occur, but the changes observed suggested a decrease in the effective ParD concentration for binding to the promoter as concluded for the gel mobility shift experiment, rather than a change in binding affinity (37). On the basis of these results, the dimeric ParD protein may be composed of two functional domains, a DNA binding domain and a ParE binding domain. Analysis of the primary amino acid sequence of ParD or ParE by using the SWISS-PROT data bank did not reveal homology to known DNA binding motifs (1).

While in vivo concentrations of the ParD and ParE proteins have not been determined, it is suspected that the *parE* gene's inefficient native TTG start codon results in production of this protein at a lower level than for the ParD protein. This may ensure a sufficiently high intracellular level of ParD to neutralize the ParE toxic activity. Thus, molar ratios of ParE′ to ParD in vitro that cause the titration of ParD away from the promoter region in gel mobility shift and footprinting assays may not be physiologically relevant. It is possible, however, that in certain instances, the intracellular ratio of ParE to ParD becomes excessively high, resulting in risk to the cell and, therefore, requiring a compensating mechanism that quickly raises the concentration of the ParD protein to correct the imbalance. For example, if a daughter cell after cell division acquires too low a level of ParD protein for full protection against the ParE protein, then removal of the bound ParD from the *parDE* promoter as observed in vitro at high ratios of ParE to ParD may be of physiological importance in derepressing the *parDE* operon to bring the ratio of the two proteins into balance.

The proximity of the *parDE* and *parCBA* operons is perhaps surprising since both operons are capable of interacting independently in the stabilization of plasmids, with *parDE* stabilizing by means of killing of plasmid-free cells and stabilization by the *parCBA* operon utilizing a mechanism that has a resolvase system as a component. The resolution of multimers, however, itself cannot account for the high level of stabilization that is observed (16, 34). To date, there is no physical evidence for interaction between these two operons at the protein or DNA level. The availability of purified ParA (11), ParD (37), and ParE′ proteins and efforts to purify the ParB and ParC proteins should yield the entire set of proteins specified by these two operons for further exploration of interactions of the various components of this stabilization system at the protein and/or DNA level.

ACKNOWLEDGMENTS

We thank Jack Dixon for the generous provision of expression vectors, Rick Roberts, George Kassavetis, and Russell Doolittle for valuable discussions, and Aresa Toukdarian and Patricia Sobecky for their critical reading of the manuscript.

This work was supported by NIH grant AIO7194. E.P.J. was supported by NIH training grant 5T32GM07317.

REFERENCES

1. **Bairoch, A., and B. Boeckmann.** 1993. The SWISS-PROT protein sequence data bank, recent developments. Nucleic Acids Res. **21:**3093–3096.
2. **Bernard, P., and M. Couturier.** 1992. Cell killing by the F plasmid CcdB protein involves poisoning of DNA-Topoisomerase II complexes. J. Mol. Biol. **226:**735–745.
3. **Bernard, P., K. E. Kézdy, L. V. Melderen, J. Steyaert, L. Wyns, M. L. Pato, P. N. Higgins, and M. Couturier.** 1993. The F plasmid CcdB protein induces efficient ATP-dependent DNA cleavage by gyrase. J. Mol. Biol. **234:**534–541.
4. **Bravo, A., G. de Torrontegui, and R. Diaz.** 1987. Identification of components of a new stability system of R1, ParD, that is close to the origin of replication of the plasmid. Mol. Gen. Genet. **210:**101–110.
5. **Bravo, A., S. Ortega, G. de Torrontegoi, and R. Diaz.** 1988. Killing of *Escherichia coli* cells modulated by components of the stability system ParD of plasmid R1. Mol. Gen. Genet. **215:**146–151.
6. **Carter, P., H. Bedouelle, and G. Winter.** 1985. Improved oligonucleotide site-directed mutagenesis using M13 vectors. Nucleic Acids Res. **13:**4431–4443.
7. **Chang, J.-Y.** 1985. Thrombin specificity: requirement for apolar amino acids adjacent to the thrombin cleavage site of polypeptide substrate. Eur. J. Biochem. **151:**217–224.
8. **Davis, T. L., D. R. Helinski, and R. C. Roberts.** 1992. Transcription and autoregulation of the stabilizing functions of broad-host-range plasmid RK2 in *Escherichia coli*, *Agrobacterium tumefaciens* and *Pseudomonas aeruginosa*. Mol. Microbiol. **6:**1981–1994.
9. **de Feyter, R., C. Wallace, and D. Lane.** 1989. Autoregulation of the *ccd* operon in the F plasmid. Mol. Gen. Genet. **218:**481–486.
10. **Eberl, L., M. Givskov, and H. Schwab.** 1992. The divergent promoters mediating transcription of the *par* locus of plasmid RP4 are subject to autoregulation. Mol. Microbiol. **6:**1969–1979.
11. **Eberl, L., C. Kristensen, M. Givskov, E. Grohmann, M. Gerlitz, and H. Schwab.** 1994. Analysis of the multimer resolution system encoded by the *parCBA* operon of broad-host-range plasmid RP4. Mol. Microbiol. **12:**131–141.
12. **Figurski, D. H., R. Meyer, and D. R. Helinski.** 1979. Suppression of ColE1 replication properties by the IncP-1 plasmid RK2 in hybrid plasmids constructed *in vitro*. J. Mol. Biol. **133:**295–318.
13. **Gerdes, K., K. Helin, O. W. Christensen, and A. Lobner-Olesen.** 1988. Translational control and differential RNA decay are key elements regulating post-segregational expression of the killer protein encoded by the *parB* locus of plasmid R1. J. Mol. Biol. **203:**119–129.
14. **Gerdes, K., P. B. Rasmussen, and S. Molin.** 1986. Unique type of plasmid maintenance function: postsegregational killing of plasmid-free cells. Proc. Natl. Acad. Sci. USA **83:**3116–3120.
15. **Gerdes, K., T. Thisted, and J. Martinussen.** 1990. Mechanism of postsegregational killing by the *hok*/*sok* system of plasmid R1: *sok* antisense RNA regulates formation of a *hok* mRNA species correlated with killing of plasmid-free cells. Mol. Microbiol. **4:**1807–1818.
16. **Gerlitz, M., O. Hrabak, and H. Schwab.** 1990. Partitioning of broad-host-range plasmid RP4 is a complex system involving site-specific recombination. J. Bacteriol. **172:**6194–6203.
17. **Grohmann, E.** 1994. Ph.D. thesis. Technischen Universität Graz, Graz, Austria.

17a. **Guan, K., and J. E. Dixon.** 1990. Eukaryotic proteins expressed in *Escherichia coli*: an improved thrombin cleavage and purification procedure of fusion proteins with glutathione-*S*-transferase. Anal. Biochem. **192:**262–267.

18. **Hakes, D. J., and J. E. Dixon.** 1992. New vectors for high level expression of recombinant proteins in bacteria. Anal. Biochem. **202:**293–298.
19. **Hiraga, S.** 1992. Chromosome and plasmid partition in *Escherichia coli*. Annu. Rev. Biochem. **61:**283–306.

20. **Hiraga, S., A. Jaffé, T. Ogura, H. Mori, and H. Takahashi.** 1986. F plasmid *ccd* mechanism in *Escherichia coli*. J. Bacteriol. **166:**100–104.
21. **Hope, I. A., and K. Struhl.** 1985. GCN4 protein, synthesized *in vitro*, binds HIS3 regulatory sequence: implications for general control of amino acid biosynthetic genes in yeast. Cell **43:**177–188.
22. **Jaffé, A., T. Ogura, and S. Hiraga.** 1985. Effects of the *ccd* function of the F plasmid on bacterial growth. J. Bacteriol. **163:**841–849.
23. **Jensen, R. B., and K. Gerdes.** 1995. Programmed cell death in bacteria: proteic plasmid stabilization systems. Mol. Microbiol. **17:**205–215.
24. **Jovanovic, O. S., E. K. Ayres, and D. H. Figurski.** 1994. Host-inhibitory functions encoded by promiscuous plasmids; transient arrest of Escherichia coli segregants that fail to inherit plasmid RK2. J. Mol. Biol. **237:**52–64.
25. **Kleiner, D., W. Paul, and M. J. Merrick.** 1988. Construction of multicopy expression vectors for regulated overproduction of proteins in *Klebsiella pneumoniae* and other enteric bacteria. J. Gen. Microbiol. **134:**1779–1784.
26. **Kyhse-Anderson, J.** 1984. Electroblotting of multiple gels: a simple apparatus without buffer tank for rapid transfer of proteins from polyacrylamide to nitrocellulose. J. Biochem. Biophys. Methods **10:**203–209.
27. **Laemmli, U. K.** 1970. Cleavage of structural proteins during the assembly of the head of bacteriophage T4. Nature (London) **227:**680–685.
28. **Lehnherr, H., E. Maguin, S. Jafri, and M. B. Yarmolinsky.** 1993. Plasmid addiction genes of bacteriophage P1: *doc*, which causes cell death on curing of prophage, and *phd*, which prevents host death when prophage is retained. J. Mol. Biol. **233:**414–428.
29. **Lehnherr, H., and M. B. Yarmolinsky.** 1995. Addiction protein Phd of plasmid prophage P1 is a substrate of the ClpXP serine protease of *Escherichia coli*. Proc. Natl. Acad. Sci. USA **92:**3274–3277.
30. **Morissey, J. H.** 1981. Silver stain for proteins in polyacrylamide gels: a modified procedure with enhanced uniform sensitivity. Anal. Biochem. **117:** 307–310.
31. **Nordström, K., and S. J. Austin.** 1989. Mechanisms that contribute to the stable segregation of plasmids. Annu. Rev. Genet. **23:**37–69.
32. **Pansegrau, W., E. Lanka, P. T. Barth, D. H. Figurski, D. G. Guiney, D. Haas, D. R. Helinski, H. Schwab, V. A. Stanisich, and C. M. Thomas.** 1994. Complete nucleotide sequence of Birmingham IncPα plasmids: compilation and comparative analysis. J. Mol. Biol. **239:**623–663.
33. **Perri, S., D. R. Helinski, and A. Toukdarian.** 1991. Interaction of plasmid-encoded replication initiation proteins with the origin of DNA replication in the broad host range plasmid RK2. J. Biol. Chem. **266:**12536–12543.
34. **Roberts, R. C.** 1992. Ph.D. thesis. University of California, San Diego.

34a. **Roberts, R. C.** Unpublished data.

35. **Roberts, R. C., R. Burioni, and D. R. Helinski.** 1990. Genetic characterization of the stabilizing functions of broad-host-range plasmid RK2. J. Bacteriol. **172:**6204–6216.
36. **Roberts, R. C., and D. R. Helinski.** 1992. Definition of a minimal plasmid stabilization system from the broad-host-range plasmid RK2. J. Bacteriol. **174:**8119–8132.
37. **Roberts, R. C., C. Spangler, and D. R. Helinski.** 1993. Characteristics and significance of DNA binding activity of plasmid stabilization protein ParD from the broad host-range plasmid RK2. J. Biol. Chem. **268:**27109–27117.
38. **Roberts, R. C., A. Ström, and D. R. Helinski.** 1994. The *parDE* operon of the broad-host-range plasmid RK2 specifies growth inhibition associated with plasmid loss. J. Mol. Biol. **237:**35–51.
39. **Ruiz-Echevarria, M. J., A. Berzal-Herranz, K. Gerdes, and R. Diaz-Orejas.** 1991. The *kis* and *kid* genes of the *parD* maintenance system of plasmid R1 form an operon that is autoregulated at the level of transcription by the co-ordinated action of the Kis and Kid proteins. Mol. Microbiol. **5:**2685–2693.
40. **Salmon, M. A., L. V. Melderen, P. Bernard, and M. Couturier.** 1994. The antidote and autoregulatory functions of the F plasmid CcdA protein: a genetic and biochemical survey. Mol. Gen. Genet. **244:**530–538.
41. **Sambrook, J., E. F. Fritsch, and T. Maniatis.** 1989. Molecular cloning: a laboratory manual, 2nd ed. Cold Spring Harbor Laboratory Press, Cold Spring Harbor, N.Y.
42. **Saurugger, P. N., O. Hrabak, H. Schwab, and R. M. Lafferty.** 1986. Mapping and cloning of the *par*-region of broad-host-range plasmid RP4. J. Biotechnol. **4:**333–343.
43. **Schagger, H., and G. von Jagow.** 1987. Tricine-sodium dodecyl sulfate-polyacrylamide gel electrophoresis for the separation of proteins in the range from 1 to 100 kDa. Anal. Biochem. **166:**368–379.
44. **Schmidt, R. J., F. A. Burr, M. J. Aukerman, and B. Burr.** 1990. Maize regulatory gene opaque-2 encodes a protein with a "leucine-zipper" motif that binds to zein DNA. Proc. Natl. Acad. Sci. USA **87:**46–50.
45. **Schwartz, R., M. H. Sommer, A. Scully, and D. H. Spector.** 1994. Site-specific binding of the human cytomegalovirus IE2 86-kilodalton protein to an early gene promoter. J. Virol. **68:**5613–5622.
46. **Sobecky, P. A., C. Easter, P. D. Bear, and D. R. Helinski.** J. Bacteriol., in press.
47. **Steyaert, J., L. V. Melderen, P. Bernard, M. H. D. Thi, R. Loris, L. Wyns, and M. Couturier.** 1993. Purification, circular dichromism analysis, crystallization and preliminary X-ray diffraction analysis of the F plasmid CcdB killer protein. J. Mol. Biol. **231:**513–515.
48. **Studier, F. W., and B. A. Moffatt.** 1986. Use of bacteriophage T7 RNA polymerase to direct selective high-level expression of cloned genes. J. Mol. Biol. **189:**113–130.
49. **Summers, D. K.** 1991. The kinetics of plasmid loss. Trends Biotechnol. **9:** 273–278.
50. **Tabor, S., and C. C. Richardson.** 1985. A bacteriophage T7 RNA polymerase/promoter system for controlled exclusive expression of specific genes. Proc. Natl. Acad. Sci. USA **82:**1074–1078.
51. **Tam, J. E., and B. C. Kline.** 1989. The F plasmid *ccd* autorepressor is a complex of CcdA and CcdB protein. Mol. Gen. Genet. **219:**26–32.
52. **Thisted, T., N. S. Sørensen, and K. Gerdes.** 1995. Mechanism of post-segregational killing: secondary structure analysis of the entire Hok mRNA from plasmid R1 suggests a fold-back structure that prevents translation and antisense RNA binding. J. Mol. Biol. **247:**859–873.
53. **Tsuchimoto, S., Y. Nishimura, and E. Ohtsubo.** 1992. The stable maintenance system *pem* of plasmid R100: degradation of PemI protein may allow PemK protein to inhibit cell growth. J. Bacteriol. **174:**4205–4211.
54. **Tsuchimoto, S., H. Ohtsubo, and E. Ohtsubo.** 1988. Two genes, *pemK* and *pemI*, responsible for stable maintenance of resistance plasmid R100. J. Bacteriol. **170:**1461–1466.
55. **Van Melderen, L. V., P. Bernard, and M. Couturier.** 1994. Lon-dependent proteolysis of CcdA is the key control for activation of CcdB in plasmid-free segregant bacteria. Mol. Microbiol. **11:**1151–1157.

55a. **Vieira, J., and J. Messing.** 1982. The pUC plasmids, an M13mp7-derived system for insertion mutagenesis and sequencing with synthetic universal primers. Gene **19:**259–263.

56. **Williams, D. R., and C. M. Thomas.** 1992. Active partitioning of bacterial plasmids. J. Gen. Microbiol. **138:**1–16.
57. **Williams, K. P., G. A. Kassavetis, and E. P. Geiduschek.** 1987. Interactions of the bacteriophage T4 gene 55 product with *Escherichia coli* RNA polymerase: competition with *Escherichia coli* σ^{70} and release from late T4 transcription complexes following initiation. J. Biol. Chem. **262:**12365–12371.
58. **Yanisch-Perron, C., J. Vieira, and J. Messing.** 1985. Improved M13 phage cloning vectors and host strains: nucleotide sequences of the M13mp18 and pUC19 vectors. Gene **33:**103–119.